The Physics of Metals and Metallography, Vol. 86, No. 3, 1998, pp. 240–249.

Description of the Behavior of a Dislocation Ensemble with Allowance for Dislocation Multiplication

M. A. Ivanov,* B. A. Greenberg, and T. O. Barabash***

* *Institute of Metal Physics, National Academy of Sciences of Ukraine, pr. Vernadskogo 36, Kiev, 252142 Ukraine*

** *Institute of Metal Physics, Ural Division, Russian Academy of Sciences, ul. S. Kovalevskoi 18, Ekaterinburg, 620219 Russia*

Received April 29, 1998

Abstract—A new approach to the description of processes of plastic deformation is developed. Within this approach, the evolution of a dislocation ensemble is determined by both dislocation multiplication and dislocation transformations with both the processes occurring against the background of elastic stresses produced by the dislocation ensemble itself. Apart from the equations of detailed balance that determine time changes in the densities of mobile (glissile) and immobile (sessile) dislocations, an equation that describes the operation of dislocation sources is suggested and a new parameter that characterizes the time of adjustment of the dislocation density to external stress is introduced. Deformation curves are analyzed at various values of the system parameters and the main features of plastic deformation for some materials are described. The nonmonotonic behavior of deformation curves that is observed in some cases upon transition from elastic to plastic deformation is suggested.

1. INTRODUCTION

Analysis of processes of plastic deformation in many cases is based on a dislocation model. A vast body of available experimental data, except for large deformations, confirms this model [1–3]. Nevertheless, many problems remain unsolved within this model; in particular, the deformation curves for some crystalline materials cannot be satisfactorily described in the whole range of stresses, including the transition from elastic to plastic behavior. The nature of the nonmonotonic dependence of $\sigma(\varepsilon)$ observed in some cases upon this transition also remains unclear. It is difficult to obtain the total set of observed shapes of deformation curves within the framework of one model. Work on the mechanisms of temperature and rate dependences of the yield stress and strain-hardening coefficient for some materials is in progress. The behavior of crystals upon multistep deformation also remains an object of discussions.

The description of plastic deformation as the evolution of a dislocation ensemble requires allowance for the most characteristic aspects of its behavior, such as dislocation multiplication and dislocation transformations. It is important that all these processes occur against the background of elastic stress fields produced by the dislocation ensemble itself. In theory, the key role is played by the relationship between the external stress and the dislocation density. The form of representation of this relationship is most controversial. But, in any case, in order that the process of plastic deformation to be established, a mutual adjustment of the applied stress and dislocation density that increases due to the operation of dislocation sources must occur. The adjustment can be very fast if the dislocation sources switch on rapidly. Otherwise, the adjustment can be extended in time. The shape of deformation curves is sensitive to the above factors and, first of all, to the characteristic time of operation of dislocation sources.

In the approach used in this work, the behavior of a dislocation ensemble is considered as the evolution of the dislocation population and is described by equations of detailed balance and equations of dislocation multiplication. We attempted to find conditions under which typical deformation curves can be obtained, such as strain-hardening curves, curves with a plateau, or $\sigma(\varepsilon)$ curves that behave nonmonotonically at small deformations, etc. We did not concretized the types of dislocation transformations, but simply divided them into transformations into long-lived and short-lived barriers and attempted to clarify how the shape of deformation curves is affected by the initial density of dislocations, temperature, deformation rate, and the characteristic time of operation of dislocation sources.

2. EQUATIONS OF DETAILED BALANCE FOR THE DISLOCATION DENSITY

The previously obtained [4, 5] equations of detailed balance that determine the mutual transformations of glissile and sessile dislocations are generalized in this work in such a manner that they could allow for not only the plastic but also elastic part of deformation.

We will represent dislocation transformations in the form of diagrams such as is shown in Fig. 1, which is constructed of two elementary diagrams. The ray diagram describes transformations of glissile dislocations into long-lived (i.e., nondestructible under certain conditions) barriers, whereas the petal-type diagram describes short-lived barriers. We used the following designations in Fig. 1: g, glissile dislocations; s, s', sessile dislocations (barriers); $\nu_{gs}\nu_{gs'}$, the frequencies of transformations of glissile dislocations into sessile dislocations (barriers); and ν_{sg}, the frequencies of the reverse transformations of barriers into glissile dislocations.

Fig. 1. Diagram of dislocation transformations.

The equations of detailed balance that determine time changes of the densities of glissile (ρ_g) and sessile (ρ_s, $\rho_{s'}$) dislocations will be written in the simplest form, assuming that these dislocation densities are uniform over the sample, i.e., are independent of the coordinates and the transformation frequencies ν_{gs}, $\nu_{gs'}$, and ν_{sg} are the averaged characteristics of the corresponding processes. Then the equations of detailed balance for the ray–petal diagram shown in Fig. 1 can be written in the following form:

$$\begin{aligned} \frac{d\rho_g}{dt} \equiv \dot{\rho}_g &= -\rho_g(\nu_{gs}+\nu_{gs'}) + \rho_s\nu_{sg} + M; \\ \dot{\rho}_s &= \rho_g\nu_{gs} - \rho_s\nu_{sg}; \\ \dot{\rho}_{s'} &= \rho_g\nu_{gs'}; \\ M = \dot{\rho}, \quad \rho &= \rho_g + \rho_s + \rho_{s'}, \end{aligned} \tag{1}$$

where $M \geq 0$ is the strength of dislocation sources.

The equations of detailed balance in the form (1) describe the behavior of a dislocation ensemble sufficiently well when the dislocations prove to be blocked along a certain length rather than locally. First of all, this is characteristic of the dislocation movement along the Peierls relief. Such blocking also occurs upon collisions of dislocations with barriers that arise as a result of reactions or with various boundaries. In intermetallic compounds, where dislocations of some orientations transform into barriers by thermal activation, blocking also occurs over a certain length rather than locally.

In notation (1) we neglect various processes that lead to a decrease in the dislocation density, such as dislocation annihilation. To describe dislocation annihilation, terms that are nonlinear in dislocation density should be added to equation (1). However, such processes can be neglected at not too high temperatures. Therefore, upon the dislocation transformations at hand, the total dislocation density can only increase or remain unaltered, i.e., $\dot{\rho} \geq 0$.

The greatest frequencies in (1) are the frequencies of the direct transformations $g \longrightarrow s, s'$ (the times of movement of a glissile dislocation until it becomes stopped at a barrier are very small). In particular, $\nu_{gs} \gg \nu_{sg}$. Since the times of observation t in processes of plastic deformation are relatively large, i.e., $t(\nu_{gs} + \nu_{gs'}) \gg 1$, the quantity $\dot{\rho}_g$ in the first of equations (1) can be neglected in comparison with $\rho_g\nu_{gs}$. It can easily be shown that in this case we have $\rho_g \ll \rho_s + \rho_{s'}$. Then, the system of equations (1) is simplified substantially and can be written in the form

$$\begin{aligned} \dot{\rho} &= \rho_g(\nu_{gs}+\nu_{gs'}) - (\rho - \rho_{s'})\nu_{sg}; \\ \dot{\rho}_{s'} &= \rho_g\nu_{gs'}, \quad \rho \approx \rho_s + \rho_{s'}. \end{aligned} \tag{2}$$

Now, we should link the densities of dislocations of various types and the frequencies of transformations with macroscopic parameters (applied stress σ, strain ε, and strain rate $\dot{\varepsilon}$). We will use the Orowan relationship, which links the rate of plastic deformation $\dot{\varepsilon}_{pl}$ and the density of glissile dislocations ρ_g (moving at a given instant)

$$\dot{\varepsilon}_{pl} = fbv\rho_{g'}, \tag{3}$$

where v is the instantaneous velocity of a moving dislocation, b is the length of the Burgers vector, and f is the Schmid factor for the slip system at hand.

The observed rate of plastic deformation $\dot{\varepsilon}$ is naturally divided into the elastic ($\dot{\varepsilon}_{el}$) and plastic ($\dot{\varepsilon}_{pl}$) parts (see, e.g., [6]):

$$\dot{\varepsilon} = \dot{\varepsilon}_{el} + \dot{\varepsilon}_{pl}, \tag{4}$$

where $\dot{\varepsilon}_{pl}$ is defined by (3), and $\dot{\varepsilon}_{el}$ can be written, using Hooke's law, in the form

$$\dot{\varepsilon}_{el} = \frac{1}{\mu}\frac{d\sigma}{dt} = \frac{1}{\mu}\frac{d\sigma}{d\varepsilon}\dot{\varepsilon}, \tag{5}$$

where μ is the effective shear modulus of the material for a given slip plane.

For the case of dynamic loading, when $\dot{\varepsilon}$ = const and $t = \varepsilon/\dot{\varepsilon}$, the system of equations (2) can be written, with allowance for (3)–(5), in the following form:

$$\begin{aligned} \frac{d\rho}{d\varepsilon} &= \frac{1}{bf\Lambda}\left(1 - \frac{1}{\mu}\frac{d\sigma}{d\varepsilon}\right) - (\rho - \rho_{s'})\frac{1}{\varepsilon_s}, \\ \frac{d\rho_{s'}}{d\varepsilon} &= \frac{1}{bf\Lambda_{s'}}\left(1 - \frac{1}{\mu}\frac{d\sigma}{d\varepsilon}\right), \end{aligned} \tag{6}$$

where

$$\Lambda^{-1} = \Lambda_s^{-1} + \Lambda_{s'}^{-1}, \quad \Lambda_s^{-1} = \nu_{gs}/v, \quad \Lambda_{s'}^{-1} = \nu_{gs'}/v, \quad \varepsilon_s = \dot{\varepsilon}/\nu_{sg}. \tag{7}$$

Observable quantities Λ_s, $\Lambda_{s'}$ (free-path lengths until stopping at corresponding barriers) and ε_s (amount of deformation over a period of $t_s = \nu_{sg}^{-1}$) are introduced instead of the transformation frequencies and the instantaneous velocity. We emphasize that two equations (6) are insufficient to find three unknown quantities ρ, $\rho_{s'}$, and σ. Therefore, we must introduce one more equation linking these quantities inaddition to (3).

3. PLASTIC FLOW CONDITIONS

For macroplastic flow to occur, it is necessary that, on the one hand, dislocation sources be operating and, on the other hand, that glissile dislocations, irrespective of the types of transformations they suffer, overcome elastic counteraction of the surroundings. We may imagine the following picture of the onset of plastic flow. Dislocation multiplication starts in preferred regions, which are isolated from one another at first. Later, these regions turn out to be connected with one another, occupying a significant portion of space, similar to how this occurs in percolation. Developing this analogy, we may assume that macrodeformation starts when a corresponding infinite (i.e., passing through the whole crystal volume) percolation cluster is developed [7]. But for this to occur, it is necessary that a certain relationship be established (and fulfilled later on) between the increasing dislocation density and the applied stress. For randomly distributed dislocations, the role of such a relation is played by the known Taylor–Seeger condition [1], when the applied stress is close to the stress produced by dislocations at average spacing between them, i.e.,

$$\sigma = k\sqrt{\rho}, \quad k = \alpha\mu b/f, \tag{8}$$

where α is a numerical coefficient.

It is obvious that condition (8) cannot be fulfilled immediately after the beginning of deformation. First of all, the external stress must exceed the quantity $k\sqrt{\rho_0}$, where ρ_0 is the initial dislocation density. Thus,

$$\sigma = \mu\varepsilon \quad \text{for} \quad \varepsilon \le \varepsilon_0, \tag{9}$$

where

$$\varepsilon_0 = \frac{k}{\mu}\sqrt{\rho_0}. \tag{10}$$

In addition, the adjustment of the dislocation density to the increasing external stress depends, according to (8), on how rapidly dislocation sources operate. The various variants of this adjustment are considered in Sections 4 and 5.

In the literature, the condition for plastic flow is frequently used (see, e.g. [8]) in a somewhat different than (8) form

$$\sigma = \sigma_F + k\sqrt{\rho}, \tag{11}$$

where σ_F is a certain starting stress, for example, the stress for a source to be switched on. Formally, we also can use this writing, since this does not lead to a loss of simplicity in the subsequent analysis. However, an analysis [9, 10] of experiments on the preliminary deformation of intermetallic compounds challenges the possibility of using relation (11).

4. DEFORMATION BEHAVIOR UPON RAPID ADJUSTMENT OF QUANTITIES ρ AND σ

4.1. Equations of Plastic Deformation

If the adjustment of the dislocation density to the applied stress occurs rapidly enough, then, given $\varepsilon \ge \varepsilon_0$, coupling condition (8) is fulfilled and can be inserted into (6). If, however, $\varepsilon < \varepsilon_0$, then the stress is described by expression (9). These two solutions join at point $\varepsilon = \varepsilon_0$.

For a further analysis, it is convenient to pass in equations (6) from the quantities ρ, $\rho_{s'}$, and σ to dimensionless quantities

$$\tilde{\rho} = \rho\frac{\alpha^2 b^2}{f^2}, \quad \tilde{\rho}_{s'} = \rho_{s'}\frac{\alpha^2 b^2}{f^2}, \quad \tilde{\sigma} = \sigma/\mu. \tag{12}$$

With these variables, the system of equations (6) takes on the following form:

$$\left.\begin{aligned} \frac{d\tilde{\rho}}{d\varepsilon} &= (\varepsilon_c + \varepsilon_{c'})\left(1 - \frac{d\tilde{\sigma}}{d\varepsilon}\right) - (\tilde{\rho} - \tilde{\rho}_{s'})\frac{1}{\varepsilon_s}, \\ \frac{d\tilde{\rho}_{s'}}{d\varepsilon} &= \varepsilon_{c'}\left(1 - \frac{d\tilde{\sigma}}{d\varepsilon}\right), \end{aligned}\right\} \quad \varepsilon \ge \varepsilon_0, \tag{13}$$

where

$$\varepsilon_c = \frac{\alpha^2}{f^3}b\Lambda_s^{-1}, \quad \varepsilon_{c'} = \frac{\alpha^2}{f^3}b\Lambda_{s'}^{-1}. \tag{14}$$

With rapidly adjusting quantities ρ and σ, the system of equations for plastic deformation includes, apart from (13), the following equations:

$$\tilde{\sigma} = \begin{cases} \varepsilon, & \varepsilon < \varepsilon_0, \quad \varepsilon_0 = \sqrt{\tilde{\rho}_0}, \\ \sqrt{\tilde{\rho}}, & \varepsilon \ge \varepsilon_0. \end{cases} \tag{15}$$

It follows directly from (15) that, upon rapid adjustment, the greater the initial dislocation density $\tilde{\rho}_0$, the greater the extension of the elastic region ε_0, which is not evident at first glance. But this is due to the fact that the greater the $\tilde{\rho}_0$, the greater the elastic counteraction of the initial dislocation structure, which must be overcome for the elastic deformation to end. The longer the free paths corresponding to various dislocation transformations, the more easily the subsequent transition to plastic flow occurs. As a result, as can be seen from (14), the values of ε_c and $\varepsilon_{c'}$ are inversely proportional to the corresponding free paths.

Thus, the behavior of a dislocation ensemble described by the system of equations (13) and (15) is determined by the above parameters ε_c and $\varepsilon_{c'}$ and the parameter ε_s (lifetime of the s-type barriers), which play the role of characteristic times and characteristic deformations, respectively.

4.2. Deformation Curves

We give solutions to system (13), (15) for some simple cases. For simplicity, we assume that the parameters ε_c, $\varepsilon_{c'}$, and ε_s are independent of the applied stress and strain.

In the case where the diagram of the ray–petal type (Fig. 1) degenerates into a ray-type diagram, which describes the $g \longrightarrow s'$ transformations into long-lived barriers, plastic deformation is defined, as follows from (13), by the simple differential equation

$$\frac{d\tilde{\sigma}^2}{d\varepsilon} = \varepsilon_{c'}\left(1 - \frac{d\tilde{\sigma}}{d\varepsilon}\right) \tag{16}$$

with the initial condition $\tilde{\sigma}_0 = \varepsilon_0$ at $\varepsilon = \varepsilon_0$.

A solution to this equation has the form

$$\frac{\tilde{\sigma}}{\varepsilon_{c'}} = -\frac{1}{2} + \frac{1}{2}\sqrt{\frac{4(\varepsilon - \varepsilon_0)}{\varepsilon_{c'}} + \left(1 + 2\frac{\varepsilon_0}{\varepsilon_{c'}}\right)^2}. \tag{17}$$

In the beginning of plastic flow, when ε differs only slightly from ε_0, i.e.,

$$\frac{\varepsilon - \varepsilon_0}{\varepsilon_{c'}} \ll \frac{1}{4}\left(1 + 2\frac{\varepsilon_0}{\varepsilon_{c'}}\right)^2, \tag{18}$$

the $\tilde{\sigma}(\varepsilon)$ dependence is linear, as for elastic deformation, but with a smaller slope equal to

$$\frac{\tilde{\sigma} - \tilde{\sigma}_0}{\varepsilon_{c'}} = \frac{\varepsilon_0}{\varepsilon_{c'}} + \frac{1}{1 + 2\frac{\varepsilon_0}{\varepsilon_{c'}}}\frac{\varepsilon - \varepsilon_0}{\varepsilon_{c'}}. \tag{19}$$

With further growth in ε, when condition (18) ceases to be valid, a changeover from linear to parabolic strain hardening occurs, according to (17),

$$\tilde{\sigma}^2 = \varepsilon\varepsilon_{c'}. \tag{20}$$

This is a consequence of the above assumption that parameter $\varepsilon_{c'}$ is independent of the stress and strain. If we assume that the free-path length $\Lambda_{s'}$ is inversely proportional to strain [1], then, using (16) and (14) for $\varepsilon_{c'}$, we obtain the stage of linear rather than parabolic strain hardening.

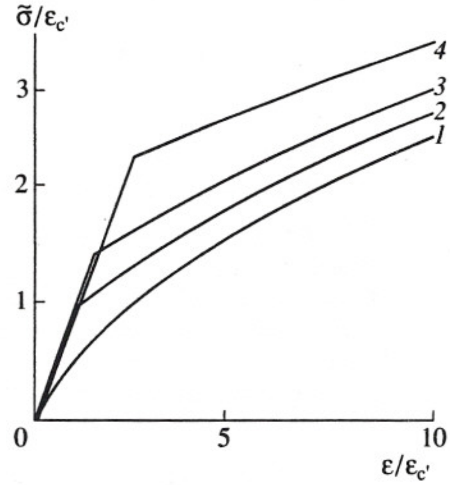

Fig. 2. Deformation curves at various initial dislocation densities $\varepsilon_0/\varepsilon_{c'}$: (*1*) 0.1; (*2*) 1.0; (*3*) 1.5; and (*4*) 2.5.

Figure 2 displays $\tilde{\sigma}(\varepsilon)$ curves that were obtained by (17) at fixed values of $\varepsilon_{c'}$ and various ε_0, i.e., various values of the initial dislocation density ρ_0. All the curves have bends at points $\varepsilon = \varepsilon_0$ and the positions of the bends increase, in accordance with (19), with increasing $\varepsilon_0/\varepsilon_{c'}$. Correspondingly, the extension of the straight (elastic) portion of the curve increases, i.e., according to (18), the changeover to the parabolic part is delayed.

At low values of ρ_0, when $\varepsilon_0/\varepsilon_{c'} \ll 1$, we obtain from (17)

$$\frac{d\tilde{\sigma}}{d\varepsilon} = 1/\sqrt{1 + 4\varepsilon/\varepsilon_{c'}}. \tag{21}$$

This means that the slope of the $\tilde{\sigma}(\varepsilon)$ curve decreases at the $\varepsilon = \varepsilon_{c'}$ point by a factor of about two in comparison with the elastic region. Thus, the parameter $\varepsilon_{c'}$ determines, on the one hand, the extension of the region of transition from elastic to plastic deformation and, on the other hand, the value of the strain-hardening coefficient upon plastic deformation.

When the ray–petal diagram degenerates into a petal-type diagram, which describes the mutual $g \longleftrightarrow s$ transformations, the equation of plastic deformation, as follows from (13), takes on the following form at $\varepsilon \geq \varepsilon_0$ (and $\sigma \geq \sigma_0$):

$$\frac{d\tilde{\sigma}^2}{d\varepsilon} = \varepsilon_c\left(1 - \frac{d\tilde{\sigma}}{d\varepsilon}\right) - \frac{\tilde{\sigma}^2}{\varepsilon_s}, \tag{22}$$

where ε_s depends, according to (7), on the strain rate $\dot{\varepsilon}$. This equation differs from (16) in the presence of a second term in the right-hand side, which becomes substantial at $\varepsilon \geq \varepsilon_s$ at the expense of reverse $s \longrightarrow g$ transformations.

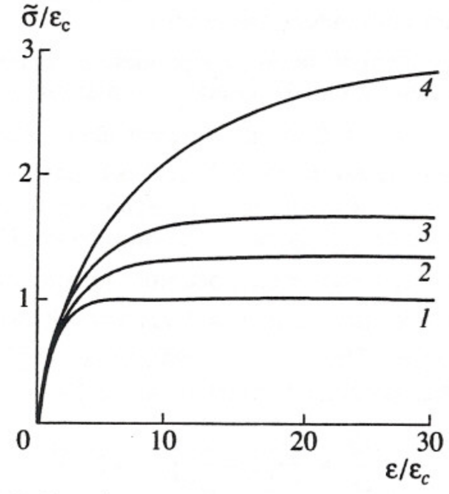

Fig. 3. Deformation curves corresponding to the petal-type diagram at various values of $\varepsilon_s/\varepsilon_c$ ($\varepsilon_0/\varepsilon_c = 0.09$): (*1*) 1.0; (*2*) 2.0; (*3*) 3.0; and (*4*) 10.0.

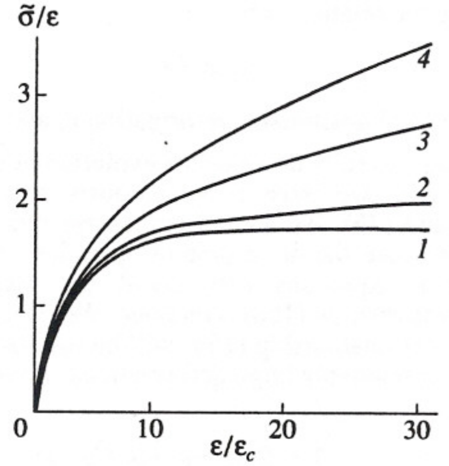

Fig. 4. Deformation curves corresponding to the diagrams of the ray–petal type at various values of $\varepsilon_{c'}/\varepsilon_c$ (at $\varepsilon_s/\varepsilon_c = 3.0$ and $\varepsilon_0/\varepsilon_c = 0.09$): (*1*) 0.00; (*2*) 0.01; (*3*) 0.05; and (*4*) 0.1.

A typical set of strain–stress curves $\tilde{\sigma}(\varepsilon)$ for different values of the $\varepsilon_s/\varepsilon_c$ ratio (for the same value of ρ_0) is given in Fig. 3.

When $\varepsilon_s \gg \varepsilon_c$, the behavior of the deformation curves in the region where $\varepsilon < \varepsilon_s$ does not differ significantly from the behavior corresponding to the ray-type diagram. In curve *4* in Fig. 3, like in curve *1* in Fig. 2, a parabolic strain-hardening stage is distinctly seen. When $\varepsilon > \varepsilon_s$, the $\tilde{\sigma}(\varepsilon)$ dependence levels off, tending to a limiting value $\tilde{\sigma}_p$ defined by the relation

$$\tilde{\sigma}_p^2 = \varepsilon_s \varepsilon_c. \tag{23}$$

When $\varepsilon_s \le \varepsilon_c$, the leveling off of the curve occurs without the stage of parabolic strain hardening (curve *1* in Fig. 3). Curves *2* and *3* illustrate the intermediate cases.

Deformation curves with plateaus (or with regions with a decreased strain-hardening coefficient) were actually observed in some materials such as semiconductors [11, 12], intermetallic compounds [13], etc. The height of the plateau decreases with decreasing strain rate and increasing temperature. Such strain-rate dependence directly follows from (23) with ε_s given by expression (7). The temperature dependence of the plateau height observed in semiconductors can be obtained if we allow for the thermoactivation character of the $s \longrightarrow g$ transformations. Indeed, in this case, the value of ν_{sg} increases exponentially with increasing temperature and, therefore, according to (7) and (23), $\tilde{\sigma}_p$ should decrease.

If we ignore the dependence of the parameters on stress, the $\tilde{\sigma}_p$ dependence on the strain rate must have a radical character, i.e., $\tilde{\sigma}_p \propto \sqrt{\dot{\varepsilon}}$, and the dependence on the reciprocal temperature must be exponential. However, the experimentally observed dependences of $\tilde{\sigma}_p$ on both $\dot{\varepsilon}$ and T are much weaker. Since the parameters (ε_s in particular) depend on stress, expression (23) can be considered only as an equation for determining $\tilde{\sigma}_p$. It can be shown that the allowance for the stress dependence of the activation energy, which determines ν_{sg}, substantially changes the form of the $\tilde{\sigma}_p(\dot{\varepsilon}, T)$ function that is a solution to equation (23). In particular, using the known expressions for the activation energy as a function of stress [1], we can obtain weaker dependences (in comparison with those considered above) of the plateau height on $\dot{\varepsilon}$ and T, close to those experimentally observed.

It should also be noted that the analysis performed in this work for the petal-type diagram is valid only for not-too-large values of the initial dislocation density, namely, when the condition

$$\tilde{\rho}_0 < \varepsilon_s \varepsilon_c \tag{24}$$

is fulfilled. The case of very high initial dislocation densities, when stress $\tilde{\sigma}_0$ is higher than the plateau height, requires separate consideration.

Since real materials always contain several types of barriers, both long-lived and short-lived, the deformation behavior can most conveniently be described by a diagram of the ray–petal type. Then the system of equations of plastic deformation has the form (13)–(15). Solutions to this set of equations for several values of the $\varepsilon_{c'}/\varepsilon_c$ ratio and fixed values of $\varepsilon_s/\varepsilon_c$ and $\varepsilon_0/\varepsilon_c$ are shown in Fig. 4. Curve *1* in Fig. 4 obtained at $\varepsilon_{c'} = 0$ coincides with curve *3* in Fig. 3 and has a plateau. At nonzero $\varepsilon_{c'}$, the deformation curves in Fig. 4, unlike those shown in Fig. 3, do not level off, but always have some slope related to $g \longrightarrow s'$ transformations. The behavior of deformation curves shows how the dominant transformations change with increasing $\varepsilon_{c'}/\varepsilon_c$ from transformations to short-lived barriers (curves with plateaus) to transformations to long-lived barriers (curves with strongly pronounced strengthening).

In all above cases, it was assumed that, immediately after the condition $\sigma = k\sqrt{\rho_0}$ is achieved, dislocation sources begin operating and the dislocation density quickly adjusts to the external stress, i.e., condition (8) is fulfilled. In what follows, we discard this assumption and consider the behavior of a dislocation ensemble with allowance for the fact that a finite time is required for dislocation multiplication.

5. DEFORMATION BEHAVIOR WITH ALLOWANCE FOR THE FINITE TIME REQUIRED FOR ADJUSTING ρ AND σ

5.1. Equations of the Evolution of a Dislocation Ensemble

It is natural to assume that the rate of dislocation formation $\dot{\rho}$ is proportional to the density of dislocation sources and, therefore, the total density of dislocations in a crystal ρ. This behavior of a dislocation ensemble permits one to draw an analogy with the evolution of other populations, e.g., biological [14]. Let us write the equation for the rate of dislocation formation in the following form:

$$\frac{d\rho}{dt} = \frac{\rho}{\tau} - A\rho^2. \tag{25}$$

Here, τ is the characteristic time that determines the operation of dislocation sources. If only the first term remained on the right-hand side of this equation, the dislocation density would grow exponentially with time (i.e., with increasing strain). It is obvious that at relatively large deformations such growth should slow down, which is described by the second term in the right-hand side of (25), proportional to the squared dislocation density. We also could take into account terms of higher orders in dislocation density, but for simplicity it is sufficient to restrict ourselves by the above summand.

Davies [15] made an attempt to link the physical nature of this summand with the mutual annihilation of dislocations. However, the annihilation processes are only important at high temperatures. At the same time, in the real dislocation ensemble there can exist other mechanisms that ensure the presence of a negative nonlinear term on the right-hand side of equation (26). First of all, this is the blocking of dislocation sources by elastic-stress fields at large dislocation densities. For biological populations, such a term corresponds to life competition, in particular, to competition for a free area. To a certain extent, the situations are similar. But for a dislocation ensemble the value of A must depend on stress, which is a specific feature of this case in comparison with other populations.

The form of the $A(\sigma)$ dependence can be found from the condition that dislocation sources are operative, i.e., $\dot{\rho} \geq 0$, only at $\tilde{\sigma} \geq \sqrt{\tilde{\rho}}$, whereas at $\sigma < \kappa\sqrt{\rho}$ the dislocation generation rate $\dot{\rho}$ becomes negative. However, if dislocation annihilation is neglected, the dislocation density can only grow or remain unaltered. Thus, when $\sigma < \kappa\sqrt{\rho}$, equation (25) becomes invalid and we should *a priori* assume that $\dot{\rho} = 0$. As a result, we obtain that $A\tau = \kappa^2/\sigma^2$. Then, at $\dot{\varepsilon} = \mathrm{const}$, equation (26) in dimensionless variables (12) takes on the form

$$\frac{d\tilde{\rho}}{d\varepsilon} = \frac{\tilde{\rho}}{\varepsilon_\tau}\left(1 - \frac{\tilde{\rho}}{\tilde{\sigma}^2}\right), \quad \tilde{\sigma} \geq \sqrt{\tilde{\rho}}; \tag{26}$$

$$\frac{d\tilde{\rho}}{d\varepsilon} = 0, \quad \tilde{\sigma} < \sqrt{\tilde{\rho}},$$

where the relationship

$$\varepsilon_\tau = \dot{\varepsilon}\tau \tag{27}$$

links the characteristic deformation ε_τ and time τ.

Thus, to fully describe the evolution of a dislocation ensemble, we must simultaneously solve equations (13) and (26). We should emphasize that with taking into account the finite time of operation of dislocation sources, equations (26) stand for relation (15b), whereas relation (15a) is retained. We can expect in this case that relationship (15b) will be fulfilled asymptotically at relatively large deformations, when $\varepsilon \gg \varepsilon_\tau$.

5.2. Deformation Curves

The set of equations that describe the evolution of a dislocation ensemble for the diagram of the ray type takes on the form

$$\left.\begin{aligned} \frac{d\tilde{\rho}}{d\varepsilon} &= \varepsilon_{c'}\left(1 - \frac{d\tilde{\sigma}}{d\varepsilon}\right), \\ \frac{d\tilde{\rho}}{d\varepsilon} &= \frac{\tilde{\rho}}{\varepsilon_\tau}\left(1 - \frac{\tilde{\rho}}{\tilde{\sigma}^2}\right), \end{aligned}\right\} \quad \tilde{\sigma} \geq \sqrt{\tilde{\rho}}; \tag{28}$$

$$d\tilde{\rho}/d\varepsilon = 0, \quad \tilde{\sigma} < \sqrt{\tilde{\rho}};$$

$$\tilde{\sigma} = \varepsilon, \quad \varepsilon < \varepsilon_0.$$

The behavior of the $\tilde{\sigma}(\varepsilon)$ and $\tilde{\rho}(\varepsilon)$ functions and their mutual adjustment depend substantially on the relationship between $\varepsilon_{c'}$ and ε_τ (see Fig. 5). When $\varepsilon_{c'} \gg \varepsilon_\tau$, we should expect a quick adjustment of the dislocation density to the external stress. Indeed, as can be seen from Fig. 5a, the condition $\tilde{\sigma} \cong \sqrt{\tilde{\rho}}$ is fulfilled right after the condition $\varepsilon \geq \varepsilon_0$ is fulfilled. In this case,

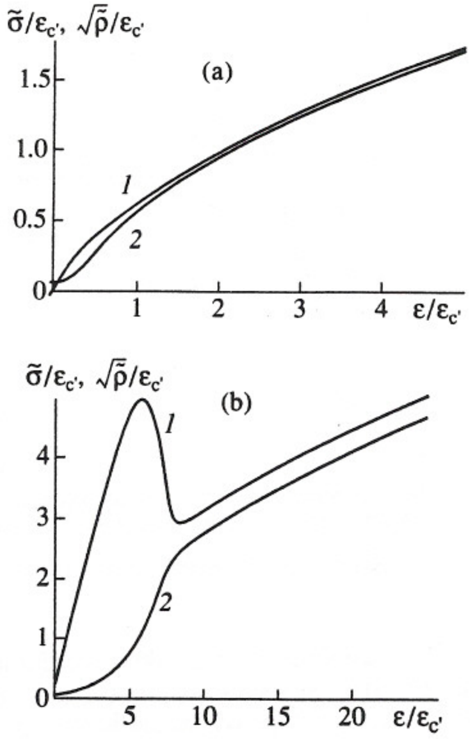

Fig. 5. External stress $\tilde{\sigma}/\varepsilon_{c'}$ (curves *1*) and the square root of dislocation density $\sqrt{\tilde{\rho}}/\varepsilon_{c'}$ (curves *2*) as functions of strain at $\varepsilon_\tau/\varepsilon_{c'}$ = (a) 0.1 and (b) 1.1 ($\varepsilon_0/\varepsilon_{c'} = 0.09$).

the value of $\sqrt{\tilde{\rho}}$ is somewhat smaller than $\tilde{\sigma}$ and at $\varepsilon \gg \varepsilon_{c'}$ their difference, according to (27), is equal to

$$\tilde{\sigma} - \sqrt{\tilde{\rho}} \cong \frac{1}{2}\tilde{\sigma}\frac{\varepsilon_\tau}{\varepsilon} \ll \tilde{\sigma}. \qquad (29)$$

It is the condition $\varepsilon_{c'} \gg \varepsilon_\tau$ that in the limiting case corresponds to the instantaneous adjustment that was considered in Section 4.

A substantially different situation can arise at large ε_τ. The typical behavior of $\tilde{\sigma}(\varepsilon)$ and $\sqrt{\tilde{\rho}(\varepsilon)}$ in this case is shown in Fig. 5b. Note the nonmonotonic dependence $\tilde{\sigma}(\varepsilon)$, which can be explained as follows. Because of the slow operation of dislocation sources, the dislocation density that is required to ensure a desired value of $\dot{\varepsilon}$ is only achieved after a certain time, i.e., at strains that are equal to or larger than ε_τ. Until this density is achieved, the desired value of $\dot{\varepsilon}$ is primarily ensured at the expense of elastic deformation and the stress takes on a relatively large value of about $\tilde{\sigma}_m \cong \varepsilon_\tau$. At deformations larger than ε_τ, the above adjustment takes place and the $\tilde{\sigma}(\varepsilon)$ dependence, in accordance with (20), becomes $\tilde{\sigma} = \sqrt{\varepsilon\varepsilon_{c'}}$. As a result, because of the transition from the linear to parabolic region in the

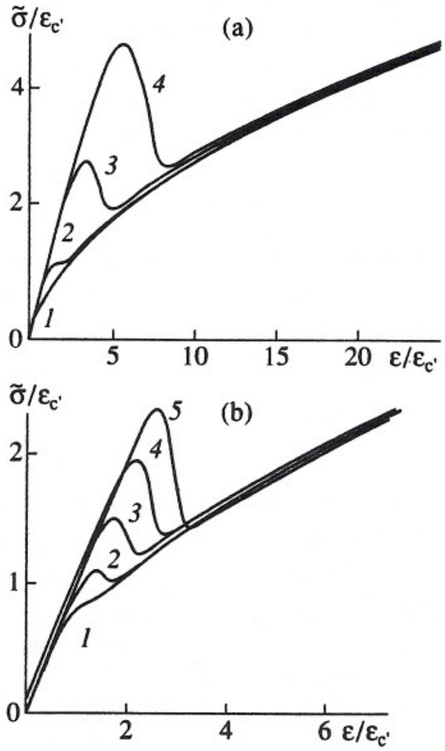

Fig. 6. Deformation curves corresponding to the ray-type diagram at various operation parameters of dislocation sources $\varepsilon_\tau/\varepsilon_{c'}$ and initial dislocation densities $\sqrt{\tilde{\rho}_0}/\varepsilon_{c'}$: (a) $\sqrt{\tilde{\rho}_0}/\varepsilon_{c'} = 0.09$, (*1*) $\varepsilon_\tau/\varepsilon_{c'} = 0.1$, (*2*) 0.3, (*3*) 0.7, and (*4*) 1.1; (b) $\varepsilon_\tau/\varepsilon_{c'} = 0.2$, (*1*) $\sqrt{\tilde{\rho}_0}/\varepsilon_{c'} = 9 \times 10^{-2}$, (*2*) 9×10^{-3}, (*3*) 9×10^{-4}, (*4*) 9×10^{-5}, and (*5*) 9×10^{-6}.

$\tilde{\sigma}(\varepsilon)$ curve, the stress must decrease with increasing ε to below $\tilde{\sigma}_m$ if the characteristic deformations ε_τ and $\varepsilon_{c'}$ are comparable in magnitudes.

Figure 6a shows a set of deformation curves for various values of the parameter $\varepsilon_\tau/\varepsilon_{c'}$. It turns out that the maximum in the $\tilde{\sigma}(\varepsilon)$ curve becomes distinct at as low values of $\varepsilon_\tau/\varepsilon_{c'}$ as 0.3 and the height of the maximum, as can be expected, increases with increasing $\varepsilon_\tau/\varepsilon_{c'}$.

Similar curves, which are solutions to the set of equations (28) at various values of the initial dislocation density $\tilde{\rho}_0$, are shown in Fig. 6b. It can be seen that the maximum height increases substantially with decreasing $\tilde{\rho}_0$. Such behavior, which is quite typical of, e.g., semiconductors [11, 12], is caused by the fact that at low initial dislocation densities a substantial time is needed to ensure a noticeable growth of the dislocation population, such that can ensure a given deformation rate $\dot{\varepsilon}$.

In addition, this explains why the maximum in deformation curves (Fig. 6a) arises at ε_τ smaller than $\varepsilon_{c'}$. Actually, the effective deformation $\varepsilon_\tau^{\text{eff}}$ that is required for adjusting dislocation density to the external stress can be represented in the form

$$\varepsilon_\tau^{\text{eff}} \approx \varepsilon_\tau \ln(\varepsilon_{c'}^2/\tilde{\rho}_0) > \varepsilon_\tau, \text{ if } \tilde{\rho}_0 \ll \varepsilon_{c'}^2. \quad (30)$$

An increase in $\varepsilon_\tau^{\text{eff}}$ with decreasing $\tilde{\rho}_0$ leads to extending the elastic portion of the deformation curve and, therefore, to increasing the maximum height which is approximately $\varepsilon_\tau^{\text{eff}}$. The condition for the occurrence of a nonmonotonic behavior of the $\tilde{\sigma}(\varepsilon)$ curve takes on the form $\varepsilon_\tau^{\text{eff}} \cong \varepsilon_{c'}$, i.e., $\varepsilon_\tau \approx \varepsilon_{c'}/\ln(\varepsilon_{c'}^2/\tilde{\rho}_0)$. As a result, the maximum appears at ε_τ that are smaller than $\varepsilon_{c'}$.

In fact, it directly follows from (30) that the extension of the elastic portion of the $\tilde{\sigma}(\varepsilon)$ curve increases with decreasing $\tilde{\rho}_0$, which does not coincide with the dependence following from (15) discussed above. However, this is only an apparent controversy. Indeed, when dislocation sources operate quickly (Section 4.1), elastic deformation continues until the deformation ε_0 is achieved at which the relationship $\tilde{\sigma}_0 = \sqrt{\tilde{\rho}_0}$ is fulfilled. Upon the slow operation of the sources, the elastic deformation continues after this condition is fulfilled until the stress reaches $\tilde{\sigma}_m$. For the curves shown in Fig. 6b, $\tilde{\sigma}_0/\varepsilon_{c'} \le 0.09$, whereas $\tilde{\sigma}_m/\varepsilon_{c'} \ge 1$.

The spreading of the elastic portion of the deformation curve caused by a very low initial dislocation density was actually observed in tests of metallic [16] and semiconducting [17] whiskers.

As follows from the above estimates, with allowance for the definition of the parameter ε_τ (27), the height of the maximum in the $\tilde{\sigma}(\varepsilon)$ curves increases and the conditions for its appearance become more favorable with increasing deformation rate $\dot{\varepsilon}$ and characteristic time τ of operation of dislocation sources, and decreasing the initial density of dislocations $\tilde{\rho}_0$.

With allowance for the $s \longrightarrow g$ transformations (diagram of the petal type), the first equation in (28) must be replaced by the following one:

$$\frac{d\tilde{\rho}}{d\varepsilon} = \varepsilon_c\left(1 - \frac{d\tilde{\sigma}}{d\varepsilon}\right) - \frac{\tilde{\rho}}{\varepsilon_s}. \quad (31)$$

Then, for $\varepsilon_c, \varepsilon_\tau \ll \varepsilon_s$, the deformation behavior in the region of $\varepsilon < \varepsilon_s$ only slightly differs from the case of long-lived barriers considered above. With further increasing ε, the deformation curve goes through the stage of parabolic strengthening and levels off, giving a plateau, as in the case when the finite time of operation of sources is neglected (see Section 4.2).

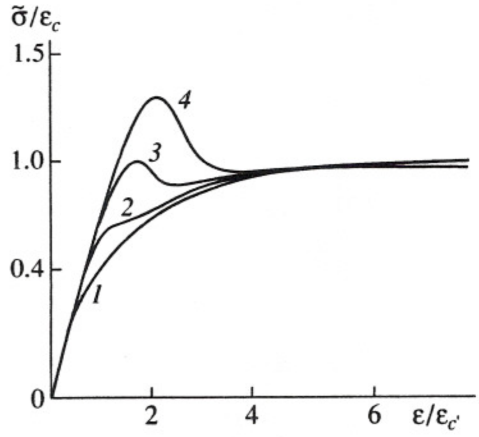

Fig. 7. Deformation curves corresponding to the petal-type diagram for various values of the parameter $\varepsilon_\tau/\varepsilon_c$ (at $\varepsilon_s/\varepsilon_c = 1$ and $\sqrt{\tilde{\rho}_0}/\varepsilon_c = 0.09$): (*1*) 0.1, (*2*) 0.2, (*3*) 0.3, (*4*) 0.4.

If, in contrast, $\varepsilon_\tau \ge \varepsilon_s$, then the deformation curve has a well-pronounced maximum and a direct leveling off (without a stage of parabolic strengthening). However, as the parameter $\varepsilon_\tau/\varepsilon_c$ increases further, the deformation curve exhibits a "break" and the stress drops below the plateau. Finally, this behavior (just as that noted in Section 4.2) is related to the assumption that plastic flow is absent at $\tilde{\sigma} < \sqrt{\tilde{\rho}}$.

The behavior of deformation curves as a function of the parameter ε_τ at comparable values of ε_s and ε_c is shown in Fig. 7. It can easily be seen how a maximum appears with increasing parameter $\varepsilon_\tau/\varepsilon_c$ in the deformation curve. The maximum height, as was noted above, is proportional to ε_τ, which, according to (28), is proportional to $\dot{\varepsilon}$ и τ. As can be seen from Fig. 7, with the parameters used, all the curves level off at the same plateau whose height is determined by expression (23). The "break" mentioned above occurs at $\varepsilon_\tau/\varepsilon_c \ge 0.45$.

As can be seen from Figs. 6b and 7, the nonmonotonic dependence $\tilde{\sigma}(\varepsilon)$ can be observed upon dislocation transformations into both long-lived and short-lived barriers. However, in both cases, the dependence of the maximum height on $\dot{\varepsilon}$ proved to be much stronger that observed experimentally [11–13]. This is related to the fact that we ignored the dependence of the parameters ε_τ, $\varepsilon_{c'}$, ε_s, and ε_c on stress. In this sense, the situation is analogous to that discussed in Section 4.2.

For an analysis of the behavior of a dislocation ensemble that is described by a ray–petal diagram, the most substantial problem is that of the change of the dominant type of dislocation transformations in the process of plastic deformation (see Section 4.2). The necessity of considering this changeover arises when describing the behavior of real systems, where several types of barriers always exist, but some of them can be overcome (or destroyed) very quickly, so that they may not manifest themselves at all in the process of deformation.

It can easily be shown that the contribution to the total stress from $g \longrightarrow s'$ transformations exceeds that from $g \longleftrightarrow s$ transformations at large deformations that satisfy the conditions $\varepsilon\varepsilon_{c'} \gg \varepsilon_s\varepsilon_c$. As was noted above, with the allowance for the finite time of operation of dislocation sources, any dislocation transformations become essential only at ε exceeding ε_τ. It is obvious therefore that the $g \longleftrightarrow s$ transformations become unobservable if the following condition is fulfilled:

$$\varepsilon_\tau\varepsilon_{c'} \gg \varepsilon_s\varepsilon_c. \quad (32)$$

In this case, we return to the ray-type diagram considered above. Since the quantities that enter into (32) depend on the temperature, deformation rate, orientation of the single crystal, etc., the conditions for the observability of dislocation transformations may change with changing these parameters.

CONCLUSION

The behavior of a dislocation ensemble in this work is described as similar to the evolution of populations. The key point uniting them is equation (25). In order to prevent the infinite growth of a dislocation ensemble or a population, the equation must contain a term that is nonlinear in density. It is natural that the mechanisms responsible for the appearance of such a term are different for a dislocation ensemble and a population. It is known that the curves describing the dependence of the population strengths on time are nonmonotonic [14].

In this work, curves with maxima were also obtained for dislocation ensembles depending on the amount of deformation, but for the behavior of stress $\tilde{\sigma}$ necessary to ensure a given deformation rate $\dot{\varepsilon}$ rather than for the dislocation density $\tilde{\rho}$. Here, a specific feature of dislocation ensembles manifests itself, which consists in that the quantities $\tilde{\rho}$ and $\tilde{\sigma}$ are related by an asymptotic relationship (15), but this relation is established only gradually, depending on whether dislocation sources operate quickly or slowly. The parameter τ in (25) is the characteristic time of operation of dislocation sources. If the quantities $\tilde{\rho}$ and $\tilde{\sigma}$ adjust instantaneously due to the rapid operation of the sources, then the $\tilde{\sigma}(\varepsilon)$ dependence virtually replicates the $\sqrt{\tilde{\rho}(\varepsilon)}$ dependence.

If the dislocation sources operate slowly, a relatively large deformation ε is necessary to obtain such a situation. At small deformations, when the above-mentioned adjustment had still no time to occur, the $\tilde{\sigma}(\varepsilon)$ dependence passes through a maximum, whereas $\sqrt{\tilde{\rho}(\varepsilon)}$ grows monotonically. Whether the adjustment occurs rapidly or slowly is determined by the above relationships between the characteristic deformation ε_τ equal to $\tau\dot{\varepsilon}$ and the quantities $\varepsilon_{c'}$, ε_c, and ε_s that characterize dislocation transformations in accordance with (7) and (14).

As the above analysis shows, the approach suggested in this paper can adequately describe the qualitative picture of plastic deformation and yields typical forms of deformation curves.

However, the condition that at $\sigma < k\sqrt{\rho}$ no plastic flow occurs at all, i.e., $\dot{\rho} = 0$, which was assumed in this work, is too rigid. In particular, it is this condition that makes it impossible to consider the case of very high initial dislocation densities for the petal-type diagrams (Section 4.2) and leads to the loss of stability of the solution to the set of equations used at large values of the parameter $\varepsilon_\tau/\varepsilon_c$ (Section 5.2). It is, therefore, natural to soften this condition and consider it as a certain approximation; in other words, it is necessary to allow for the spread of the condition of dislocation percolation through a dislocation framework. We think that this will eliminate the arising difficulties.

One of the most important problems in considering processes of plastic deformation is also an analysis of stress required for switching dislocation sources on. This problem is of particular importance for intermetallic compounds that exhibit anomalous temperature dependence of the yield stress [18]. Therefore, the stress of switching dislocation sources on also must be appropriately included into the scheme under consideration.

ACKNOWLEDGMENTS

This work was supported by the Russian Foundation for Basic Research (projects nos. 95-02-05656, 97-02-26671, and 98-02-17278) and the Ukrainian Foundation for Basic Research (project no. F4/128-97).

REFERENCES

1. Berner, R. and Kronmüller, H., *Plastische Verformung von Einkristallen* (Plastic Deformation of Single Crystals), Berlin: Springer, 1965.
2. Basinski, S.J. and Basinski, Z.S., Plastic Deformation and Work Hardening, in *Dislocation in Solids: Dislocations in Metallurgy*, Nabarro, F.R.N., Ed., Amsterdam: North-Holland, 1979, vol. 4, ch. 16, pp. 261–362.
3. Rollest, A.D. and Kocks, U.F., A Review of the Stages of Work Hardening, in *Dislocations 93*, Rabier, J. *et al.*, Eds., Geneva: Scitec, 1994, pp. 1–18.
4. Greenberg, B.A. and Ivanov, M.A., New Concepts of Analyzing Plastic Deformation of TiAl and Ni_3Al Intermetallic Compounds, *Mater. Sci. Eng., A*, 1992, vol. 153, pp. 356–363.
5. Greenberg, B.A. and Ivanov, M.A., Dominant Dislocation Transformations and Temperature Dependence of Flow Stress in Intermetallic Compounds, *Phys. Met. Metallogr.*, 1994, vol. 78, no. 3, pp. 247–265.

6. Saada, G., Plastic Deformation and Dynamical Systems., *Dislocations 93*, Rabier, J. *et al.*, Eds., Geneva: Scitec, 1994, pp. 87–100.
7. Stauffer, D., Scaling Theory of Percolation Clusters, *Phys. Rep.*, 1979, vol. 54, no. 1, pp. 1–74.
8. Ezz, S. and Hirsh, P.B., The Effect of Room Temperature Deformation on the Yield Stress Anomaly in $Ni_3(AlHf)B$, *Philos. Mag. A*, 1996, vol. 73, no. 4, pp. 1069–1082.
9. Greenberg, B.A., Ivanov, M.A., Barabash, T.O., and Blokhin, A.G., Comparative Analysis of Stress Jumps in Metals and Intermetallic Compounds: I. Description of Two-Stage Straining; II. Stress Macrojumps, *Phys. Met. Metallogr.*, 1996, vol. 81, no. 4, pp. 374–380, 381-386.
10. Greenberg, B.A. and Ivanov, M.A., Theoretical Description of the Two-Step Deformation of Intermetallics, *Mat. Sci. Eng., A*, 1997, vol. 240, pp. 813–818.
11. Alexander, H., Dislocations in Covalent Crystals., in *Dislocations in Solids*, Nabarro, F.R.N., Ed., Amsterdam: Elsevier, 1986, vol. 7, ch. 35, pp. 113–234.
12. Rabier, J. *et al.*, Dislocations and Plasticity in Semiconductors, *Rev. Phys. Appl.*, 1987, vol. 22, no. 11, pp. 1327–1351.
13. Suzuki, T., Mishima, Y., and Miura, S., Plastic Behaviour in Ni1(Al,X)—Temperature, Strain Rate, Orientation, and Composition, *ISIJ Int.*, 1989, vol. 29, no. 1, pp. 1–23.
14. Haken, H., *Synergetics*, Heidelberg: Springer, 1978.
15. Davies, C.H.J., Dynamics of the Evolution of the Dislocation Populations, *Scr. Metall. Mater.*, 1994, vol. 30, no. 3, pp. 349–353.
16. Honeycombe, R.W.K., *The Plastic Deformation of Metals*, London: Arnold, 1968.
17. Rhodes, R.G., *Imperfections and Active Centres in Semiconductors*, Oxford: Pergamon, 1964.
18. Greenberg, B.A. and Ivanov, M.A., Blocking of Dislocations and Dislocation Sources in TiAl, in *Gamma Titanium Aluminides (ISGTA '95)*, Y.-W. Kim *et al.*, Eds., Warrendale, PA: The Metallurgical Soc., 1995, pp. 299–305.